Measurement of ductile fracture evolution in sheet metal forming

M. Sasso, M. Rossi, G. Chiappini, D. Amodio
DIISM, Università Politecnica delle Marche, Ancona (Italy)
m.sasso@univpm.it

ABSTRACT. The present work aims to develop a method for evaluating the strain field of an object, mainly a sheet metal, up to the very edge of an eventual discontinuity in its surface. The study originates from the need of measuring the strains in sheet metals that underwent stamping process or Nakazima tests, where cracks occurred. In such cases, the investigation method typically used, that is the optical grid method, is likely to fail just where more interesting data could be captured, because of the discontinuity in the surface. From this starting point, authors borrowed and modified the XFEM approach, where enriched shape functions are used to describe the internal displacement fields of finite elements.

SOMMARIO. Il presente lavoro mira a sviluppare un metodo per valutare il campo di deformazione di un oggetto, principalmente una lamiera, fino al bordo di un eventuale discontinuità nella sua superficie. Lo studio nasce dalla necessità di misurare le deformazioni in lamiere in cui si sono verificate delle criccature durante il processo di stampaggio o durante prove di tipo Nakazima. In tali casi è probabile che il metodo di indagine tipicamente utilizzato, cioè il metodo ottico di griglia, fallisca proprio dove si trovano i dati più interessanti a causa della discontinuità nella superficie. Da questo punto di partenza, gli autori hanno preso in prestito e modificato l'approccio XFEM, dove vengono usate funzioni di forma arricchite per descrivere i campi di spostamento interno di elementi finiti in presenza di discontinuità.

KEYWORDS. Optical grid method; Extended finite element; Sheet metal stamping.

INTRODUCTION

The work represents an attempt of improving the optical method named "grid method" usually adopted to evaluate the strain fields in stamped sheet metals.

The optical grid method consists in applying a regular pattern of markers onto a surface before it is deformed by some forming process. Sometimes, especially in the early or manual versions of the method, ink circles are used, that deforms and turns into ellipses giving a straight visual evaluation of the principal strains; measuring the axis lengths provide a quantitative measure as well. However, the pattern most often consists of evenly spaced dots or intersecting lines, with each dots or line cross representing the markers. This technique is well suited to be automated and, as such, adopted in commercial system.

In experimental mechanics nowadays, more appealing techniques are present for the full field measurement of displacements and strains; in particular the digital image correlation (DIC) is by far the most employed method both in laboratory [1, 2] and industrial environments [3]. Its advantages mainly lies in the ease of surface preparation with a relatively high accuracy and resolution.

Comparatively, the grid method appears quite outmoded and obsolete from certain point of view; nevertheless, still exist application where DIC cannot be employed, such as the sheet metal stamping and, actually, all the processes where the material cannot be observed during the deformation course.
This work originates from the need of measuring the strain field in a stamped part for automotive application (see Fig. 1); in such a situation, the only applicable technique is the grid method since the object cannot be framed during the process and no image correlation could be carried out. Typically, a stereoscopic camera system is used to compute the 3D coordinates of the markers onto the deformed surface; then, by knowledge of their positions in the undeformed configuration, actual strains in the framework of large displacement can be computed [4,5].
Considering the stamped part in Fig. 1, the large crack observed in the central region actually prevents from measuring the strains in the most revealing region, where a comparison with FEM analyses would provide a useful insight for the process engineering.
In the following of the paper, a possible method for extending the measure of the strain by optical grid method up to the crack edge is numerically assessed, inspiring by the enrichment formulation used in the xFem approach [6].

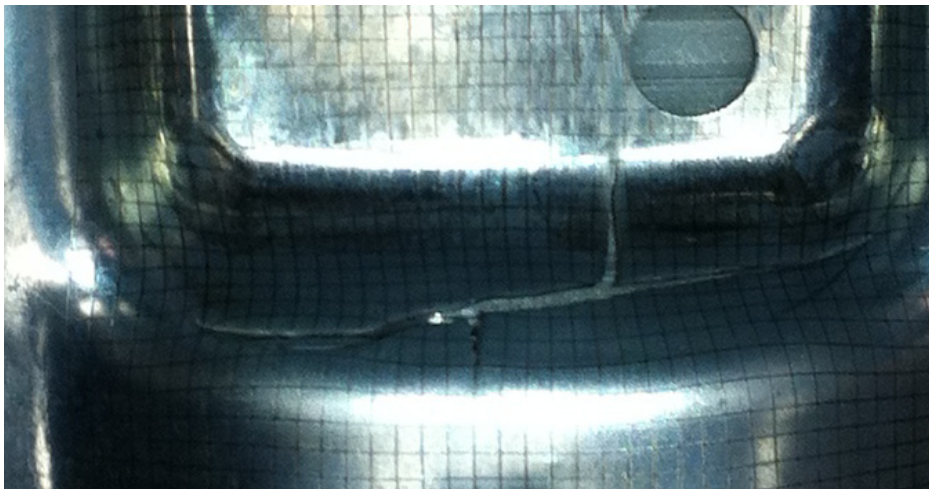

Figure 1: Cracked stamped part with grid pattern.

BASIC CONCEPTS IN OPTICAL GRID METHOD

The main steps of this technique can be described as follows: a grid of known size is impressed on the sheet blank before stamping; the grid, after being deformed during the forming process, is acquired by means of two high resolution cameras which have been previously calibrated in a common reference frame.
The markers, that is the grid intersections, are automatically recognized by means of blob analysis and a stereoscopic algorithm is used to computed their 3D coordinates X in an absolute reference frame. Considering a 4 nodes element, the natural coordinates U and V are used to fit the acquired markers positions X and the undeformed, regularly spaced, coordinates X^0:

$$X^0(U,V)=\sum_{n=1}^{4} X_i^0\,\varphi_i(U,V) \qquad \text{for the undeformed configuration} \qquad (1a)$$

$$X(U,V)=\sum_{n=1}^{4} X_i\,\varphi_i(U,V) \qquad \text{for the deformed configuration} \qquad (1b)$$

where $\varphi_i(U,V)$ are the four bilinear shape functions representing the partition of unity within the element domain.

Accordingly to the continuum mechanics theory [7] for large strain, the strain gradient tensors, containing the partial derivatives of the shape functions, shall be introduced:

$$F^0_{pq} = \frac{\partial X^0_p}{\partial U_q} \qquad \text{for the undeformed configuration} \qquad (2a)$$

$$F_{pq} = \frac{\partial X_p}{\partial U_q} \qquad \text{for the deformed configuration} \qquad (2b)$$

The logarithmic principal strains on a tangent plane are computed solving the eigenvalue problem:

$$\varepsilon_{1,2} = \log \sqrt{eig\left[\left(F^{0T}F_0\right)^{-1} F^T F\right]} \qquad (3)$$

while the third strain is computed by assuming the isochoric hypothesis.

SHAPE FUNCTIONS ENRICHMENT

Clearly, the elements of the grid that are cut by the crack in Fig. 1, cannot be processed anymore with the simple formulation explained above; indeed, the nodes lying at opposite sides of the crack experimented large displacement which are not related to the internal deformation of the element, since the continuity of the internal displacement is not satisfied.
In such cases, the pioneering work of Belytshcko provided a valuable tool for studying the displacement and strain distribution in proximity of cracks without remeshing or without defining a specialized mesh. This approach, named Extended Finite Element Method (xFem) which has been already adopted with some success to DIC method [8].
At least to the author knowledge, no such extension has been yet attempted on the grid method, which is characterized by the fact that the mesh cannot be chosen in anyway (it is given by the measured points) and only the deformed and undeformed configurations are known, without any information of intermediate steps.
The problem of the internal displacements within a FE mesh where one or more elements are cut by a crack is stated as in the following equation:

$$X(U,V) = \sum_{i\in I} X_i \varphi_i(U,V) + \sum_{j\in J} b_j \varphi_j(U,V) H(U,V) + \sum_{k\in K} \varphi_k(U,V)\left[\sum_{l=1}^{4} c^l_k F_l(U,V)\right] \qquad (4)$$

in which J is the set of nodes of the elements that are completely cut by a crack, K is the set of nodes of the elements containing crack tips, H is a discontinuous or jump function, give for example, but not necessarily, by

$$H(U,V) = \begin{cases} +1 & \textit{for upper subelement} \\ -1 & \textit{for lower subelement} \end{cases} \qquad (5)$$

The functions F_l are enrichment shape functions that contain the filed discontinuity that one desire to take into account. In [6], 4 functions are suggested for approximating the displacement field close the crack tip, namely

$$\left\{F_l(U,V)\right\} = \left\{\sqrt{r}\sin\frac{\theta}{2}, \sqrt{r}\cos\frac{\theta}{2}, \sqrt{r}\sin\frac{\theta}{2}\sin\theta, \sqrt{r}\cos\frac{\theta}{2}\sin\theta\right\} \qquad (6)$$

where r and θ are the local polar coordinates of a given point with respect to the crack tip. The nodes set are illustrated in Fig. 2.
Considering for example a single square element of unit side length, subjected to membranal displacements, a possible deformed shape, with an internal through crack, is the red one shown in Fig. 3. The four corners of the element could be regarded to as the markers of a regular grid impressed onto the planar sheet metal before the stamping; in this way, the coordinates of the four corners are known in both undeformed and deformed (e.g. by photogrammetry or other optical techniques) configurations. On the contrary, the coordinates of the mid-side nodes cut by the crack still can be measured in the deformed configuration (finding for example the intersection between the grid lines and the crack edge), but are not

known in the undeformed configuration; for this reason, the typical grid method implemented in commercial instruments, cannot provide a result in the elements or region that are cut by the crack.

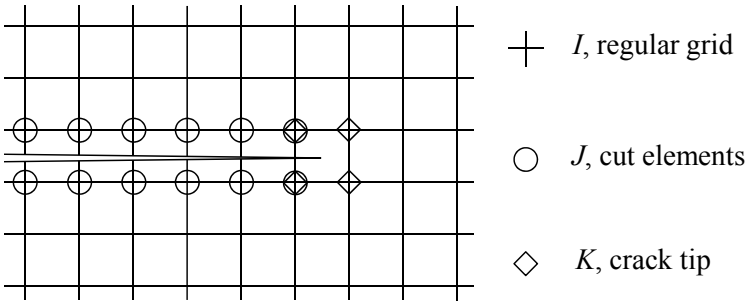

Figure 2: Enrichment configuration.

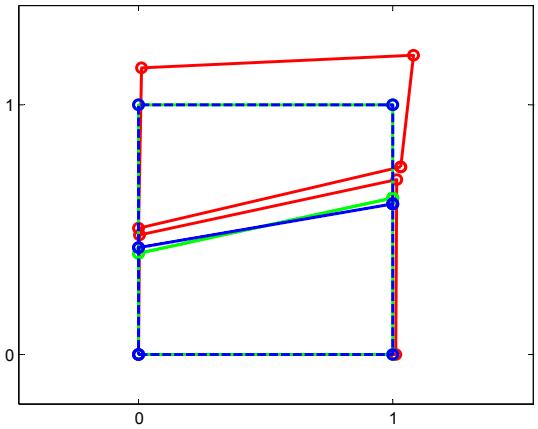

Figure 3: Square element: deformed (red) and undeformed (blue: based on strain energy, green: based on strain difference)

In this work the authors propose a method, here named xGrid, to extend the measurement, with some hypothesis and approximations, to the free edges of the crack. The idea lies in guessing and then optimizing the position of the mid-side nodes in the undeformed configuration according to some minimization criteria. For doing this, the typical bilinear shape functions that are used in quadrangular elements must be modified. We borrowed the enrichment shape functions used in the xFem formulation for taking into account the discontinuity in the displacement field when passing from one sub-element to the other. The optimization criteria may vary from application to application; here two similar approaches have been adopted and compared: the former involves the minimization of the global strain energy, the latter consists in minimizing the strain difference (in a tensorial sense) between the conjugate boundaries of the two sub-elements.

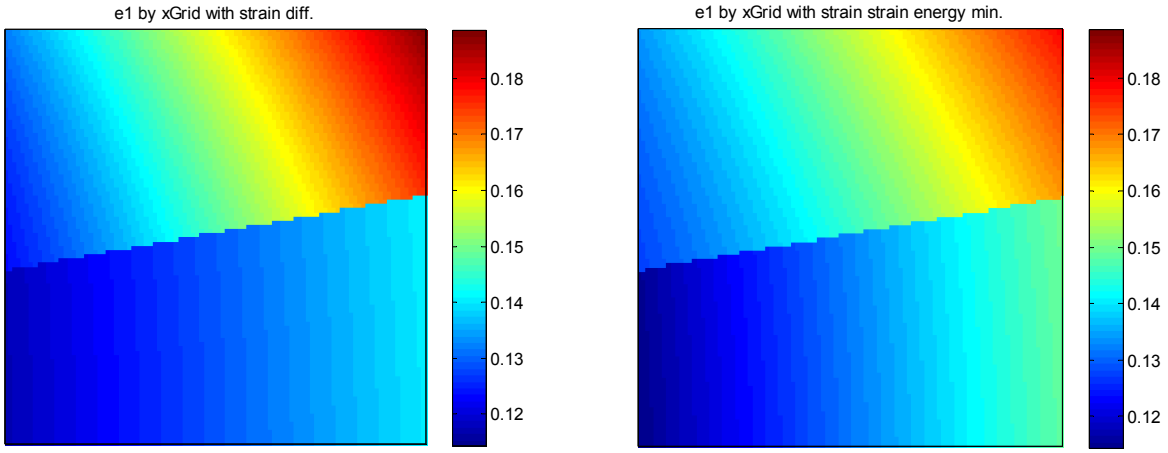

Figure 4: Difference in the first principal strain maps between the two minimization criteria.

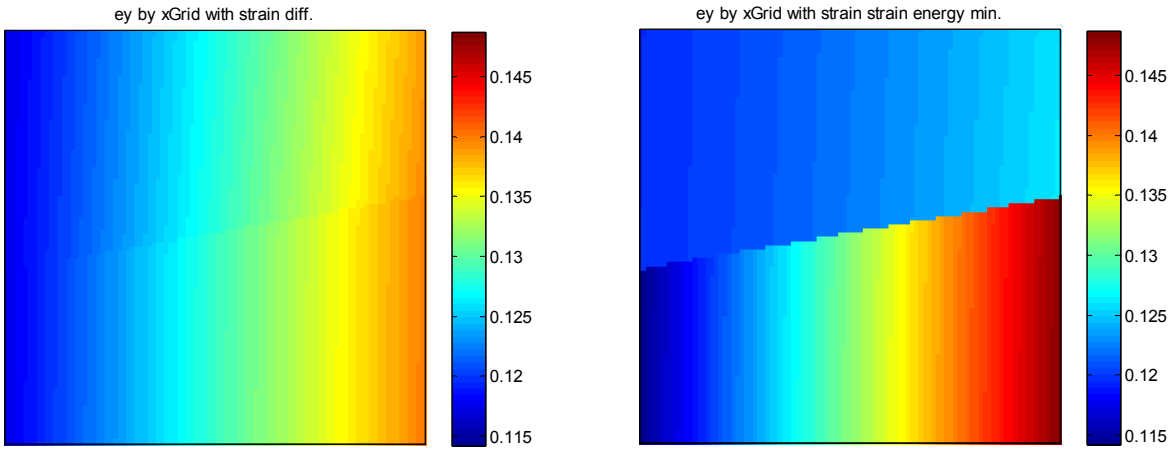

Figure 5: Difference in the Y strain maps between the two minimization criteria

Both methods permit to compute the strain field up to the free edges of the through crack; this already represents an upgrading of the classical grid method where the elements cut by the crack are inevitably omitted from the strain computation. However, depending on the nodal displacements, they are likely to provide quite similar results, as shown in Fig. 4; sometimes some difference in the estimations of the strain distribution may arise, as shown in Fig. 5.

FE MODEL OF A CRACKED STAMPED PANEL

The FE model reproduced a 1 mm thick sheet metal which is deformed by a spherical bulge coming from the bottom. The sheet metal is a square of 100 mm size, whose material properties are reported in Tab. 1; the rigid punch has a radius of 20 mm and is moved upward of 25 mm after the initial contact occurs at the bottom surface of the sheet metal.

E [GPa]	υ	E_T [MPa]	σ_Y [MPa]
200	0.27	1000	200

Table 1: The specimen's material properties.

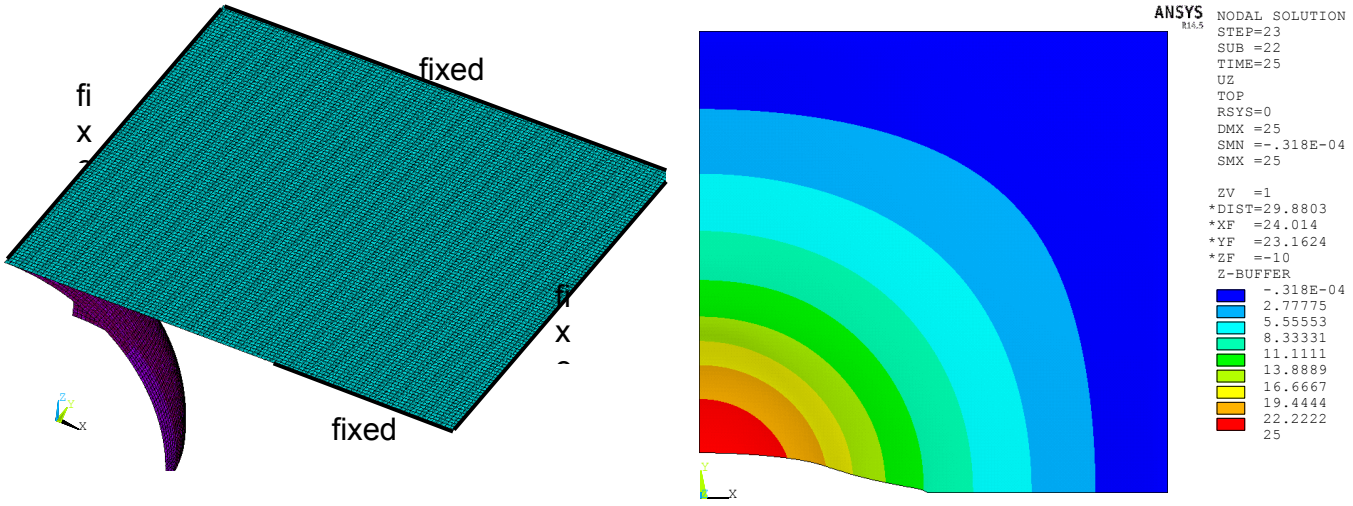

a) b)

Figure 6: FE model, a) mesh and constraints, b) resulting out-of-plane displacements

The sheet metal has been modelled with shell 43 elements, 0.5 mm in size, by means of Ansys® software, exploiting the double symmetry with respect to x and y axes(see Fig. 6a). The nodes at the external sides were fixed, while the nodes on the internal side obeyed the symmetry conditions, exception made for the nodes from the centre to the x=24 mm coordinate, that was constrained in the y direction by means of uniaxial non-linear springs; the springs have an almost infinite stiffness up to 205 N, then their stiffness vanishes. In this way it was possible to reproduce a plausible fracture initiation and propagation, with accumulation of plastic strain at the crack edges, without the need for element kill (which would correspond to material loss). The nodal results of this simulation computed at the middle of the shell thickness, see Fig. 6b, were used as a virtual object to be acquired by means of optical grid method, both the classical one and the eXtended method here proposed.

VIRTUAL EXPERIMENT BY OPTICAL GRID METHOD

As aforementioned, the FE results were used to simulate a real object. The distribution first principal strain as computed by the fine meshed FE simulation, mapped onto the undeformed configuration and viewed from the top, is shown in Fig. 7. Here, for the sake of comprehensibility, the entire maps are shown without symmetry.

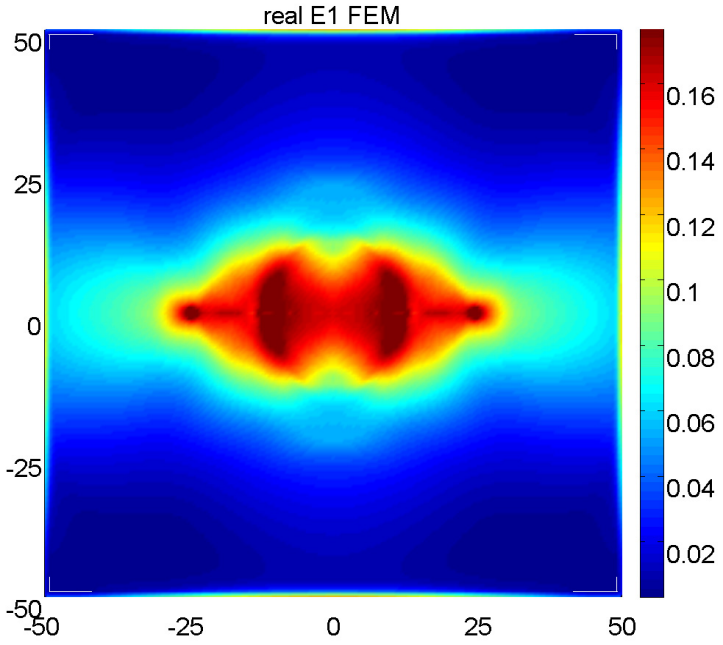

Figure 7**:** "real" strain distribution map as computed by FEM with fine mesh

If now the FEM shape and strains are considered as real, the nodal data can be "sub-sampled" thus to simulate what would happen in the optical grid method, where the markers are evenly spaced in the undeformed configuration; here a regular grid of 4 mm pitch is considered. This sub-sampling results inevitably in a sort low-pass filter of the real data, with the stronger gradient and peak values being smoothed. Fig. 8 show example of results, in terms of the first principal strain, with the grid parallel to the crack (a) and with a rotation of 20° and 3mm offset in Y direction (b). The virtual markers grid is superimposed for clarity. The missing areas correspond to the elements that are cut by the grid. Since everything has been mapped onto the undeformed configuration, it is now possible to perform a simple point-by-point subtraction of these data from the real ones given in Fig. 7. The error maps are shown in Fig. 9a and 9b.
It is observed that the grid method, because of the pitch size, provides quite accurate results where the strain gradient are small, but the error increases when the strain concentrates, with an underestimation of 2-3 % in the yellow areas; at the crack tip the error is even greater but this part is not considered in this work.
In the same way, the distribution maps of the first principal strain have been computed by the eXtended grid method procedure here presented, using the strain difference minimization criteria. The maps are shown in Fig. 10. Now, only the 2 elements containing the crack tips are omitted from the computation. The filled areas appear to provide acceptable

results; indeed, analyzing the error maps of Fig. 11 it is noted that the error level remains in the same range of Fig. 9. In particular, the error in the elements cut by the crack and at the crack edge are of the same order, or even lower, than the typical error due to "sub-sampling" shown in Fig. 9.

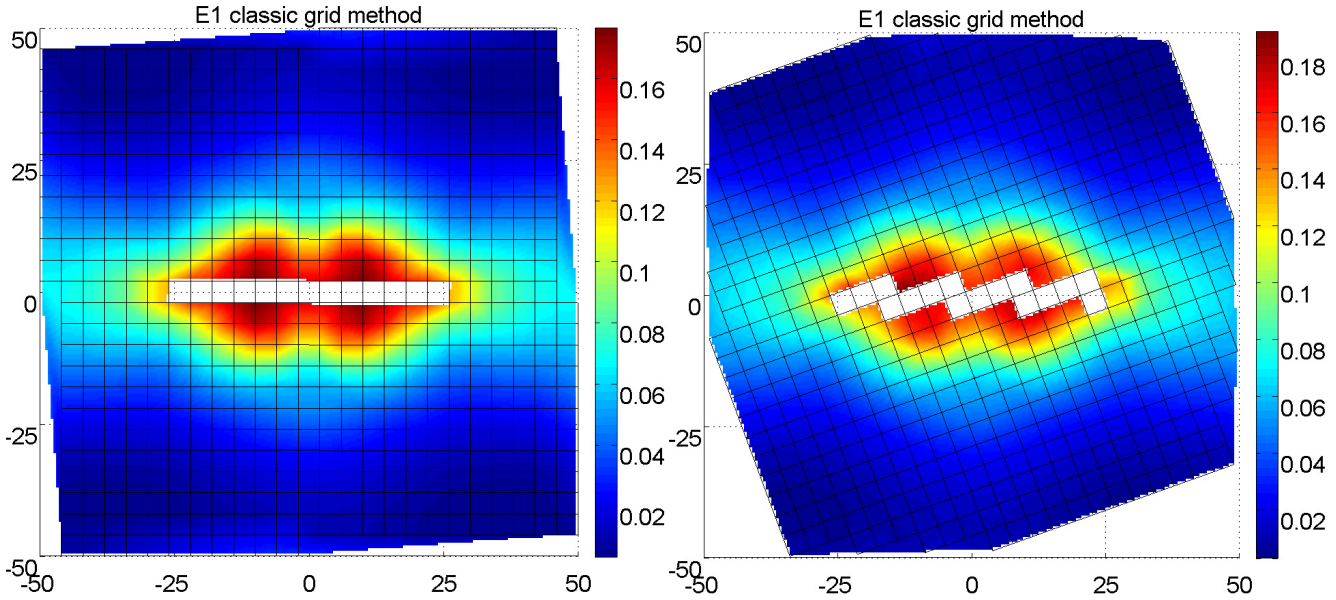

Figure 8: ε_1 distribution map for a simulated grid method of pitch 4 mm, a) crack parallel, b) 20° rotated.

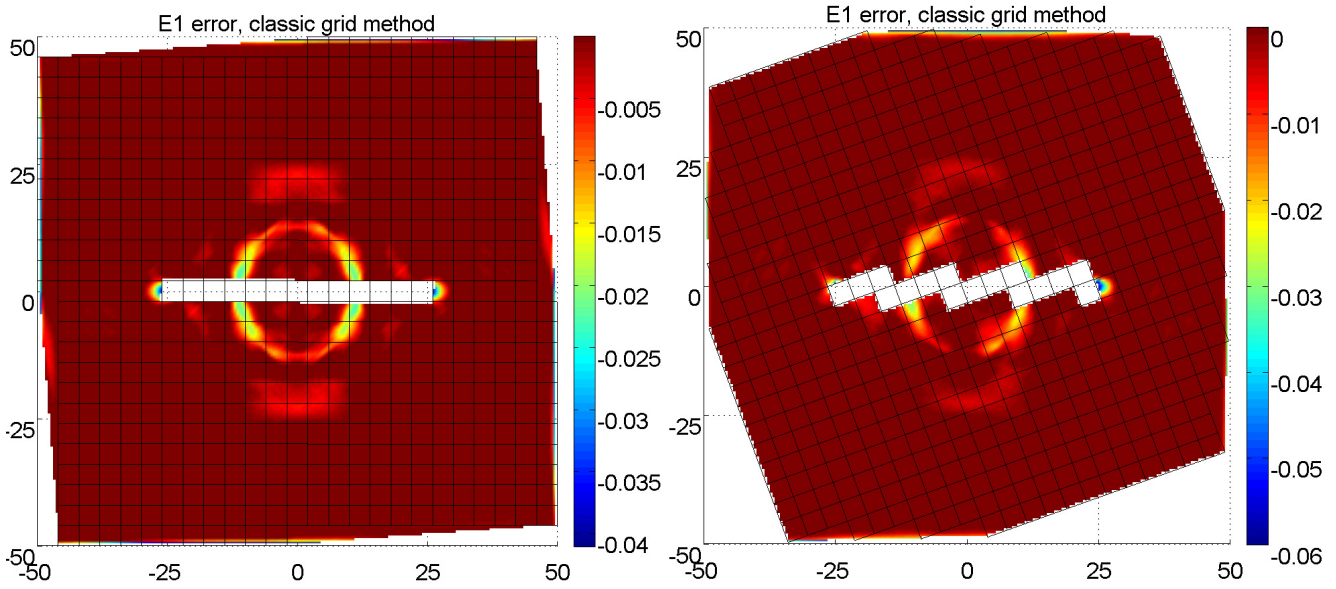

Figure 9: ε_1 error map for a simulated grid method of pitch 4 mm, a) crack parallel, b) 30° rotated.

CONCLUSIONS

The xFem approach, based on the utilization of enriched shape functions for taking into account the discontinuities in the displacement fields, has been implemented in a simulated grid method procedure, aiming to extract information on the strain levels up to crack edges. The first results of this eXtended grid method, appears encouraging for further study. In particular, the elements with a through crack provided excellent matching with the source FEM data; next step of the work may try to include the elements containing the crack tips in the procedure.

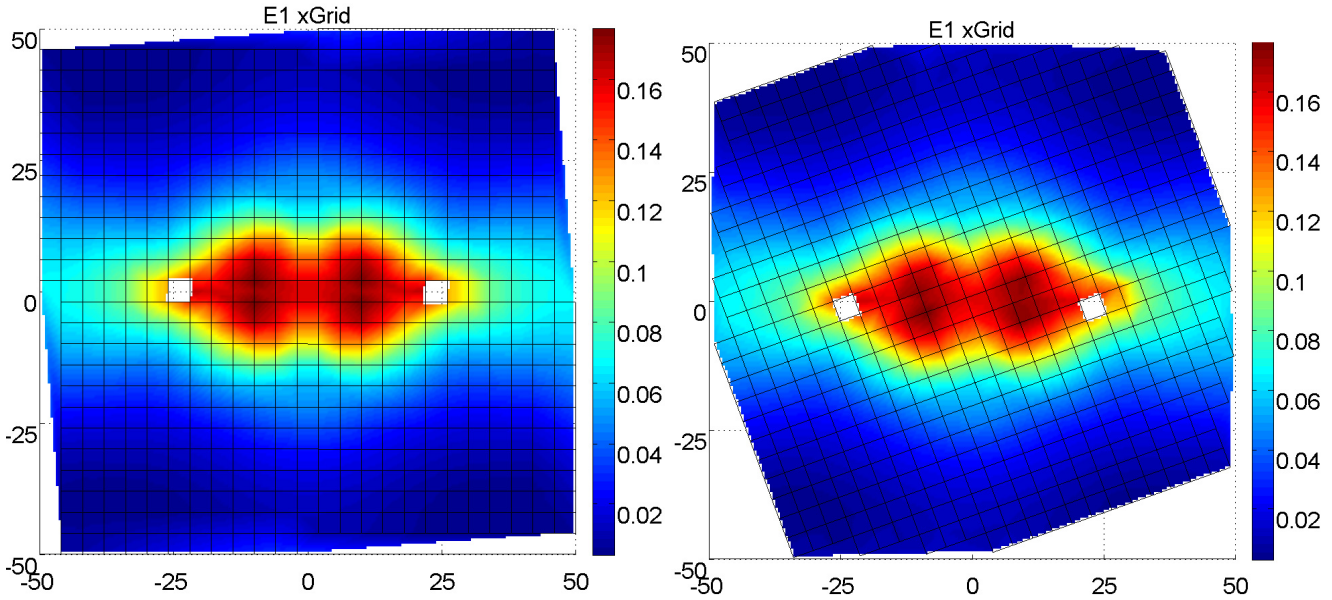

Figure 10: ε_1 distribution map for the simulated eXtended grid method of pitch 4 mm, a) crack parallel, b) 20° rotated.

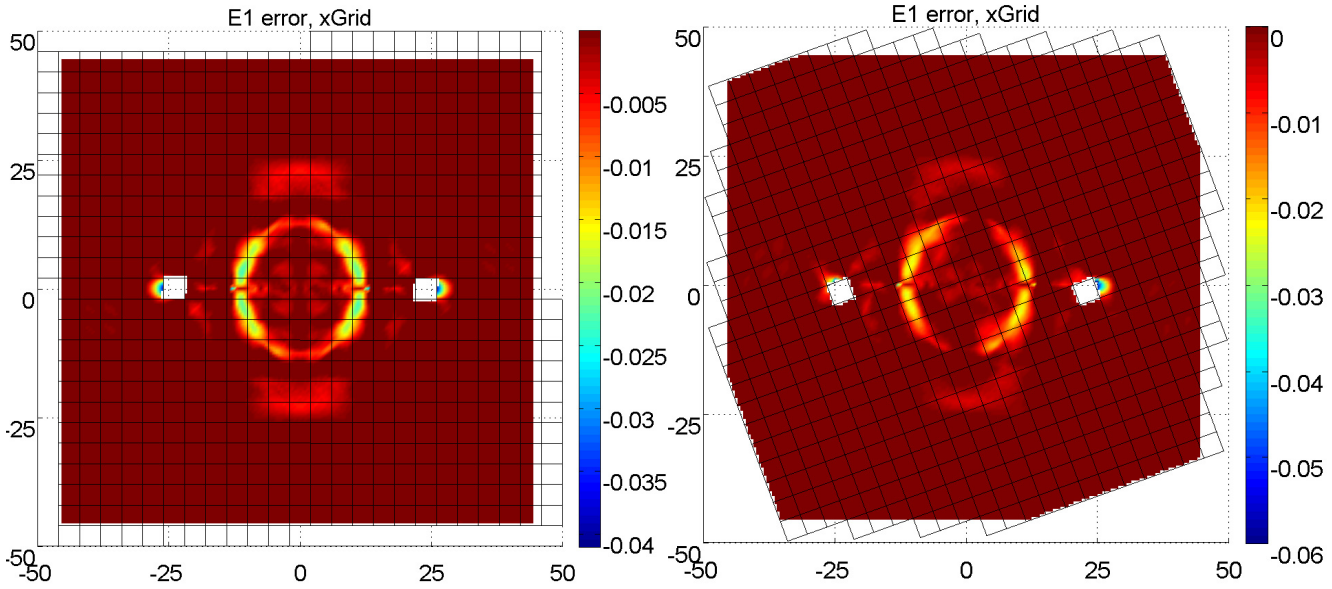

Figure 11: ε_1 error map for the simulated eXtended grid method of pitch 4 mm, a) crack parallel, b) 30° rotated.

REFERENCES

[1] G. Palmieri, M. Sasso, G. Chiappini, D. Amodio, Strain, 47(2) (2011) 196.
[2] G. Chiappini, M. Sasso, M. Rossi, In: Proc. SEM 2012 Annual Conference, 3 (2012) 173.
[3] M.A. Sutton, J.J. Orteu, H.W. Shreier, Image correlation for shape, motion and deformation measurement: basic concepts, theory and applications, Springer, (2009).
[4] M. Sasso, M. Callegari, D. Amodio, Meccanica, 43 (2008) 153.
[5] M. Sasso, D. Amodio, In: Proc. SEM 2006 Annual conference, 3 (2006) 1161.
[6] M. Nicholas, J. Dolbow, T. Belytschko, Int. J. Numer. Meth. Engng., 46 (1999) 131.
[7] T.J. Chung, Continuum Mechanics, Prentice Hall International, Englewood Cliffs (1988).
[8] J. Réthoré, F. Hild, S. Roux, Int. J. Numer. Meth. Engng., 73 (2008) 248.